Journal of Engineering Mathematics 18 (1984) 335–349.

Reflection of a weak shock wave from a perforated plug

J.F. CLARKE

Department of Aerodynamics, College of Aeronautics, Cranfield Institute of Technology, Cranfield, Bedford MK43 0AL, UK

(Received August 20, 1984)

Summary

A plane shock wave is assumed to be incident upon a solid surface that is perforated by a number of closely spaced holes of length L and radius a, where $a/L \ll 1$, and the problem is to determine the character of the reflected wave field. The latter is essentially determined when the rate of inflow from the ambient atmosphere to the perforated plug is known, and the majority of the effort in this paper is devoted to the evaluation of this quantity. The assumption that the incident wave is weak is made throughout. Results show how the reflected wave field depends upon L and a and upon the acoustic-impedance ratio of the ambient air and the air within the slender tubes; the latter may be influenced by the distensibility of the tubes, although this matter is not pursued here. It is theoretically possible for reflected-shock strengths to exceed the solid-wall value for short intervals of time. Qualitative comparisons of the present theory with some existing observations of rather strong-shock reflection from perforated plugs lend support to the predictions, especially in the situation for which viscous effects are slight.

1. Introduction

Consider the situation sketched in Fig. 1, which depicts a large tube whose end is closed by a plug. The plug is perforated to a constant depth by a large array of closely-packed slender holes. A shock-wave is incident on the perforated plug from the air-filled region above it, and a number of questions now arise. For example, what is the strength of the reflected wave and how does it vary with time? Is there a secondary reflected shock or shocks arising from the presence of a second reflecting surface at the base of the slender holes? How are these factors influenced by the radius and length of the holes?

Apart from the intrinsic interest of the problem there are some potential practical applications of the configuration that should be mentioned. For example the perforated plug can be thought of as a structurally robust absorber of blast waves. The analysis to be described below will be restricted to weak incident waves; these are included in a large class of real blast phenomena, arising from the discharge of weapons, the rupture of pressure vessels and similar sources whose reflections are undesirable; one may need to use a wave-cancellation device that has some structural rigidity in order to cope with these problems.

The configuration and its behaviour has some connection with the behaviour of randomly-porous materials, although this important topic is taken up in detail elsewhere (Clarke [2]). It is sometimes useful to be able to create a controlled disturbance in the nominally stagnant gas behind a shock that is reflected from the closed end of a shock

tube, and the perforated-plug (or bundle of hypodermic needles) is one way in which this can be accomplished quite simply. A practical example of this technique is to be found in Scott's [6] studies of fully-dispersed shock waves in shock-heated carbon dioxide.

The first part of the present paper in Sec. 2 deals with the disturbance flow in a single tube of small diameter-to-length ratio. It is assumed that the motion of the air in such a tube can be modelled as a one-dimensional unsteady polytropic compressible flow of small amplitude, with viscous resistance to this motion described by an average friction-factor expression that is linearly proportional to local gas velocity. Laplace transform methods are used to find a disturbance-pressure/inflow-velocity relation at the upper, interface, end of a tube (see Fig. 1). Nonlinear weak-wave propagation in the free atmosphere above the perforated plug (Fig. 1) is analysed briefly in Sec. 3 and the problem is formally solved by making the resulting disturbance-pressure/inflow-velocity relationship compatible with conditions at the end of the aggregation of slender tubes. In particular it is required that both pressure and mass-flux shall be continuous at the interface, and this latter condition introduces the geometric "openness ratio" factor σ, defined as the fraction of the upper surface area of the plug that is penetrated by the collection of holes.

The result of this analysis, at the end of Sec. 3, is an expression in Laplace-transform form for the inflow velocity from the atmosphere to the plug. Since this transform cannot be inverted simply a number of special cases and some matters of analytical interest are

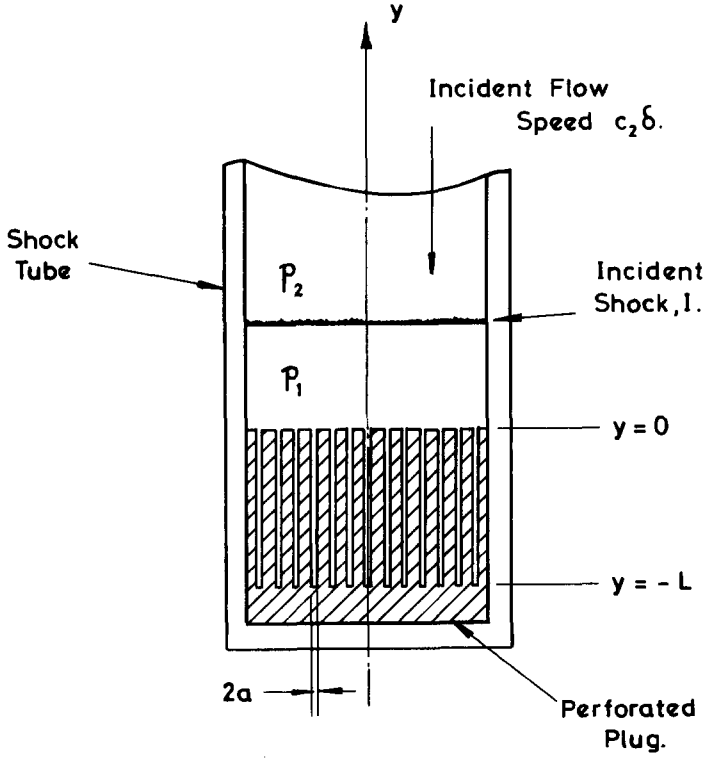

Figure 1. The incident shock-wave I approaching the perforated plug. The slender tubes are of length L and radius a. Pressure ahead of the incident wave and within the tubes prior to time $t = 0$ is p_1; downstream of I the pressure is p_2 and the incident-flow speed is $c_2\delta$, where c_2 is the sound speed behind I and δ is a small number.

described in Sec. 4. The former are principally useful for purposes of comparison with the main results, that are finally acquired by simple numerical quadrature; they also make clear the role played by waves reflected from the base of the perforations. The results discussed in Sec. 5 reveal the rather complicated parts played by hole diameter and length, viscosity and openness ratio, and the paper concludes with a comparison between the present theory and Scott's [6] observations of a situation for which viscous effects are weak.

2. Transient behaviour in a slender tube

It will be assumed that the flow in a long slender tube can be treated as a one-dimensional unsteady process and that, with v' as the average flow velocity within the tube, the viscous resistance to motion produces a force per unit volume that is equal to v'/α, where

$$\alpha = a^2/8\mu, \tag{2.1}$$

and μ is the (constant) viscosity coefficient; a is the tube's radius. It will be assumed that the flow-velocity v' is small compared with the local sound speed and one can therefore linearise the inertia term in the momentum equation which now reads

$$\rho_c v'_t = -\hat{p}_y - \frac{1}{\alpha} v', \tag{2.2}$$ *

where ρ_c is a constant mean value of the density and $\hat{p}$ is the mean pressure in a tube cross-section. It will subsequently be seen to be useful to identify density in this way, instead of making an immediate identification of ρ_c with the mean density of the air in the atmosphere outside the tubes. A combination of the mass-conservation equation and a polytropic relation (p proportional to ρ^n) leads to the equation

$$\hat{p}_t = -np_c v'_y, \tag{2.3}$$

where p_c is a constant mean value of $\hat{p}$ that is of course related to ρ_c. Equations (2.2) and (2.3) now constitute two equations for the two unknowns, pressure $\hat{p}$ and velocity v'.

Consider the initial-value problem that has v' zero and $\hat{p}$ equal to the constant value p_1 (see Fig. 1) everywhere in $0 > y \geqslant -L$; L is the length of a single tube within the plug and it will be assumed that at $y = -L$ the tube is closed, so that $v'(t, -L) = 0$.Denote by an overbar the Laplace transform with respect to t of $(\hat{p} - p_1) \equiv p'$ and v' as follows;

$$(\bar{p}', \bar{v}') = \int_0^\infty (p', v') e^{-st} dt. \tag{2.4}$$

It can then be shown that (2.2), (2.3) and the condition $\bar{v}'(s, -L) = 0$ (which is the transform version of $v'(t, -L) = 0$) give rise to the relation

$$\bar{v}'_w = -\frac{f(s)}{\rho_c(s + \alpha')} \tanh(f(s)L)\, \bar{p}'_w, \tag{2.5}$$

* Equation (2.2) is the momentum equation, linearised for small perturbations from a suitable mean condition, and with a simple bulk estimate for viscous resistance, in the usual spirit of one-dimensional unsteady gas dynamics.

where $\bar{v}'_w$ and $\bar{p}'_w$ are the values of $\bar{v}'$ and $\bar{p}'$ at $y = 0-$, and α' is defined as follows:

$$\alpha' \equiv 1/\rho_c \alpha. \tag{2.6}$$

Also

$$cf(s) \equiv \{s(s+\alpha')\}^{1/2}, \tag{2.7a}$$

$$c \equiv (np_c/\rho_c)^{1/2}. \tag{2.7b}$$

Equation (2.5) provides a relationship between gas velocity and pressure at the open end of a single tube. Note that c, defined in (2.7b), is a polytropic sound speed for the air within the tubes.

Equation (2.5) enables one to calculate v'_w or p'_w as a function of time t once either p'_w or v'_w is prescribed. The dynamics of gaseous behaviour in the free space above the plug will provide another relation between pressure and velocity, whence the problem is formally completed once one has made a connection between these pressure and velocity values and the ones that appear in (2.5). It will be assumed that pressure is continuous in the neighbourhood of the interface $y = 0$, and in particular that

$$p'(t, 0-) \equiv p'_w = p(t, 0+) - p_1, \tag{2.8}$$

where $p(t, y > 0)$ is the absolute pressure in $y > 0$. Only a fraction $\sigma (0 \leqslant \sigma \leqslant 1)$ of the interface at $y = 0$ is open so that one must write

$$\sigma v'(t, 0-) \equiv \sigma v'_w = v(t, 0+) \tag{2.9}$$

since mass must not accumulate at the interface. (This relation assumes continuity of density across $y = 0$, with implications for the value of ρ_c; the matter will be raised and discussed again below.) Therefore (2.5) can be translated into a relation between p and v as y approaches zero from above; i.e. the boundary condition for the external gas flow is now

$$\bar{v}_w = -\sigma f(s) \rho_c^{-1} (s+\alpha')^{-1} \tanh(f(s)L) \overline{(p_w - p_1)}. \tag{2.10}$$

It will be useful to write (2.10) in the short form

$$\bar{v}_w = -G(s) \overline{(p_w - p_1)}, \tag{2.11}$$

where $G(s)$ is defined to be

$$\begin{aligned} G(s) &\equiv \sigma f(s) \rho_c^{-1} (s+\alpha')^{-1} \tanh(f(s)L), \\ &= \frac{\sigma s^{1/2} \tanh\left\{ s^{1/2} \left(\rho_c s + \alpha^{-1}\right)^{1/2} L (np_c)^{-1/2} \right\}}{(np_c)^{1/2} \left(\rho_c s + \alpha^{-1}\right)^{1/2}}. \end{aligned} \tag{2.12}$$

3. The formal solution of the problem

The behaviour of pressures and velocities in an unsteady one-dimensional flow of small velocity-amplitude is well known (e.g. Whitham [7], §9.1) and need not be re-calculated here. The necessary results of the analysis are listed below. First, the local pressure and velocity can be written as follows;

$$p \sim p_2 + \delta p^{(1)}, \quad v \sim -c_2\delta + \delta v^{(1)}, \tag{3.1}$$

where the parameter δ is defined in Fig. 1. Multiplication of δ by c_2, the sound speed in the flow behind the incident shock wave, gives the incident flow velocity towards $y = 0$. Pressure and velocity perturbations are related as follows

$$p^{(1)} = \rho_2 c_2 v^{(1)}. \tag{3.2}$$

Finally the solution for $v^{(1)}$ is given in the parametric form

$$v^{(1)} = v_w^{(1)}(\beta), \tag{3.3}$$

$$c_2 t - y = \beta - \left\{\tfrac{1}{2}(\gamma+1)\left(v_w^{(1)}(\beta)/c_2\right) - 1\right\} y\delta, \tag{3.4}$$

where $v_w^{(1)}$ is the value of $v^{(1)}$ at $y = 0+$ and γ is the (constant) ratio of specific heats. At this stage $v_w^{(1)}$ is a function to be found for $\beta > 0$; since there is no disturbance prior to time $t = 0$ it is already known that

$$v_w^{(1)}(\beta < 0) = 0. \tag{3.5}$$

Evaluation of $v_w^{(1)}$ proceeds as follows. Using (3.1) and (3.2) as well as the Laplace transform with respect to t in (2.11) shows that

$$-c_2\delta s^{-1} + \delta\bar{v}_w^{(1)} = -G(s)\left\{(p_2 - p_1)s^{-1} + \delta\rho_2 c_2 \bar{v}_w^{(1)}\right\}.$$

Noting that the incident shock is weak, by hypothesis, so that

$$p_2 - p_1 \simeq \rho_2 c_2^2 \delta, \tag{3.6}$$

it follows that

$$v_w^{(1)} = \frac{c_2}{s}\left\{\frac{1 - \rho_2 c_2 G(s)}{1 + \rho_2 c_2 G(s)}\right\}. \tag{3.7}$$

The solution is now formally complete because (3.7) can be inverted to give $v_w^{(1)}(t)$ for $t > 0$ and hence, of course, $v_w^{(1)}(\beta > 0)$. Inversion of the Laplace transform is described in the next section. Meanwhile it should be noted that when ρ_c is zero the function $G(s)$ in (2.12) reduces to

$$G_0(s) = \sigma(s\alpha/np_c)^{1/2} \tanh\left\{(s/np_c\alpha)^{1/2} L\right\}.$$

A little manipulation soon shows that (3.7) is formally identical with (4.4) in Clarke's [3]

paper; in other words when the inertia term is ignored, (2.2) reduces to Darcy's law and the earlier results are therefore recovered.

The behaviour of $v_w^{(1)}$ as $t \to 0+$ can be ascertained by examining (3.7) in the limit as $|s| \to \infty$. Equation (2.12) shows that

$$G(s \to \infty) \to \sigma/(np_c\rho_c)^{1/2} = \sigma/\rho_c c,$$

where c is defined in (2.7b). Therefore (3.7) implies that

$$v_w^{(1)}(0+) = c_2\left(\frac{1-r}{1+r}\right) \tag{3.8}$$

where r, defined by

$$r \equiv \sigma(\rho_2 c_2/\rho_c c), \tag{3.9}$$

is the open-ness factor σ modified by the acoustic-impedance ratio of the air outside and inside the slender tubes. If $\rho_c \to 0$, $r \to \infty$ and $v_w^{(1)}(0+) \to -c_2$, which is precisely the result obtained from the inertialess model (Clarke [3]). Having used the freedom to choose ρ_c arbitrarily as a device to check the present analysis and relate it to earlier work, it should be noted that, in view of the postulated weakness of the incident shock, the physical reality is that ρ_c will be essentially the same as the mean value of density throughout the field, namely ρ_2. Thus a physically acceptable value for r is

$$r = \sigma(c_2/c), \tag{3.10a}$$

or if, as is highly likely, c is synonymous with c_2, then

$$r = \sigma. \tag{3.10b}$$

The matter will be raised again in Secs. 4 and 5 after some more detailed results have been obtained.

4. The inflow function

The solution of the problem is only complete when (3.7) has been inverted or, in other words, when the integral

$$\frac{1}{c_2}v_w^{(1)}(t) \equiv V = \frac{1}{2\pi i}\int_{Br}\frac{1}{s}\left\{\frac{1-\rho_2 c_2 G(s)}{1+\rho_2 c_2 G(s)}\right\}e^{ts}ds \tag{4.1}$$

has been evaluated. V is defined here for the sake of brevity later on; Br is the Bromwich inversion contour, that lies parallel to the Im(s) axis and to the right of all singularities of the integrand in (4.1). With the definition of r in (3.9), (4.1) can be re-written with the aid of (2.12) in the following form

$$V = \frac{1}{2\pi i}\int_{Br}\frac{1}{z}\left\{\frac{(z+1)^{1/2} - rz^{1/2}\tanh\left(\bar{\alpha}L[z(z+1)]^{1/2}\right)}{(z+1)^{1/2} + rz^{1/2}\tanh\left(\bar{\alpha}L[z(z+1)]^{1/2}\right)}\right\}e^{c_2 t\bar{\alpha}z}dz \tag{4.2}$$

where

$$\bar{\alpha} = 1/\alpha\rho_2 c_2, \tag{4.3}$$

The Laplace transform in (4.2) is not listed in any of the available tables of Laplace transforms, and so the integral must be evaluated here. It will be helpful to examine one or two special cases to start with.

(i) The case $L = \infty$.

Suppose that L is infinite, then the integrand in (4.2) simplifies somewhat, and one can write $V = V_\infty$, where

$$V_\infty = \frac{1}{2\pi \mathrm{i}} \int_{Br} \frac{1}{z} \left\{ \frac{(z+1)^{1/2} - z^{1/2} r}{(z+1)^{1/2} + z^{1/2} r} \right\} \mathrm{e}^{c_2 t \bar{\alpha} z} dz, \tag{4.4}$$

Now suppose that $r = 1$ and re-write (4.4) as follows, where $V_{\infty 1}$ is the value of V_∞ when $r = 1$; then

$$V_{\infty 1} = 1 - 2e^{-c_2 t\bar{\alpha}/2} \frac{1}{2\pi \mathrm{i}} \int_{Br} \left\{ \frac{(w + \frac{1}{2})^{1/2}}{(w - \frac{1}{2})^{1/2}} - 1 \right\} \mathrm{e}^{c_2 t \bar{\alpha} w} dw.$$

This last integral can be found from inverse Laplace transform number (2.4) in §5.3 of Erdélyi et al. [4], so that

$$V_{\infty 1} = 1 - \exp(-c_2 t\bar{\alpha}/2)\left[I_0(c_2 t\bar{\alpha}/2) + I_1(c_2 t\bar{\alpha}/2) \right], \tag{4.5}$$

where I_n, $n = 0, 1$, is the modified Bessel function of the first kind of order n. It is interesting to note the connection between $\bar{\alpha}$ here and a parameter $\hat{A}^2$ that appears in a related paper on porous-media behaviour (Clarke [2], particularly Appendix A). This relationship is

$$\bar{\alpha} = r^2 \hat{A}^2 \tag{4.6}$$

and it will prove helpful to present some subsequent results here in terms of $\hat{A}^2$.

When $r \neq 1$ one must resort to numerical evaluation of (4.4). Note that the integrand in (4.4) has branch points at $z = 0$ and -1, and no poles. It is therefore possible to deform Br into a small closed curve surrounding the two branch points and thus to show that

$$V_\infty = 1 - \frac{4r}{\pi} \int_0^1 \frac{(1 - w^2)^{1/2} \mathrm{e}^{-c_2 t r^2 \hat{A}^2 w^2}}{(1 - (1 - r^2) w^2)} dw. \tag{4.7}$$

The relation (4.6) is incorporated in (4.7) because it is particularly useful to illustrate V_∞ as a function of $c_2 t\hat{A}^2$ for given values of r, rather than as a function of $t\bar{\alpha}$. It is instructive to include the curve for $v_w^{(1)}$ when $r = \infty$, and flow in the tubes is inertia-less, in such

comparisons. Reverting to (4.4), and noting (4.6), change the variable of integration from z to s/r^2; then

$$V_\infty = 1 - \frac{1}{2\pi i}\int_{Br}\left\{s^{1/2}\left(s^{1/2}+\left(1+s/r^2\right)^{1/2}\right)\right\}^{-1} 2\exp\left(c_2 t\hat{A}^2 s\right)ds.$$

When $r \to \infty$ the integrand approaches $2\{s^{1/2}(s^{1/2}+1)\}^{-1}\exp(c_2 t\hat{A}^2 s)$ and V_∞ takes the value $V_{\infty\infty}$, where

$$V_{\infty\infty} = 1 - 2\exp\left(c_2 t\hat{A}^2\right)\mathrm{erfc}\left(\hat{A}(c_2 t)^{1/2}\right). \tag{4.8}$$

This result is strictly comparable with one previously found by the writer [3] for the inertia-less version of (2.2); i.e. $\rho_c \to 0$, and note (3.9). Expression (4.8) is plotted in Fig. 2 as a full line for comparison with the Simpson's-rule evaluations of (4.7) for $r = 0.4$, $\frac{2}{3}$, 0.8, 1&2. It should be remarked that the numerical estimates for the integral when $r = 1$ agree very well with a direct evaluation of $V_{\infty 1}$ from (4.5) using Table 9.8, page 416, from Abramowitz and Stegun [1]. Because it can be measured experimentally $v_w/c_2\delta$ is plotted in Fig. 2. From (3.1) and (4.1) it can be seen that this quantity is simply $(V-1)$. Note that $c_2 t\hat{A}^2$ is the natural dimensionless group for the time-variable t in the limiting (inertia-less) case, $r \to \infty$. Plotting results for finite values of r against this same variable, as in Fig. 2,

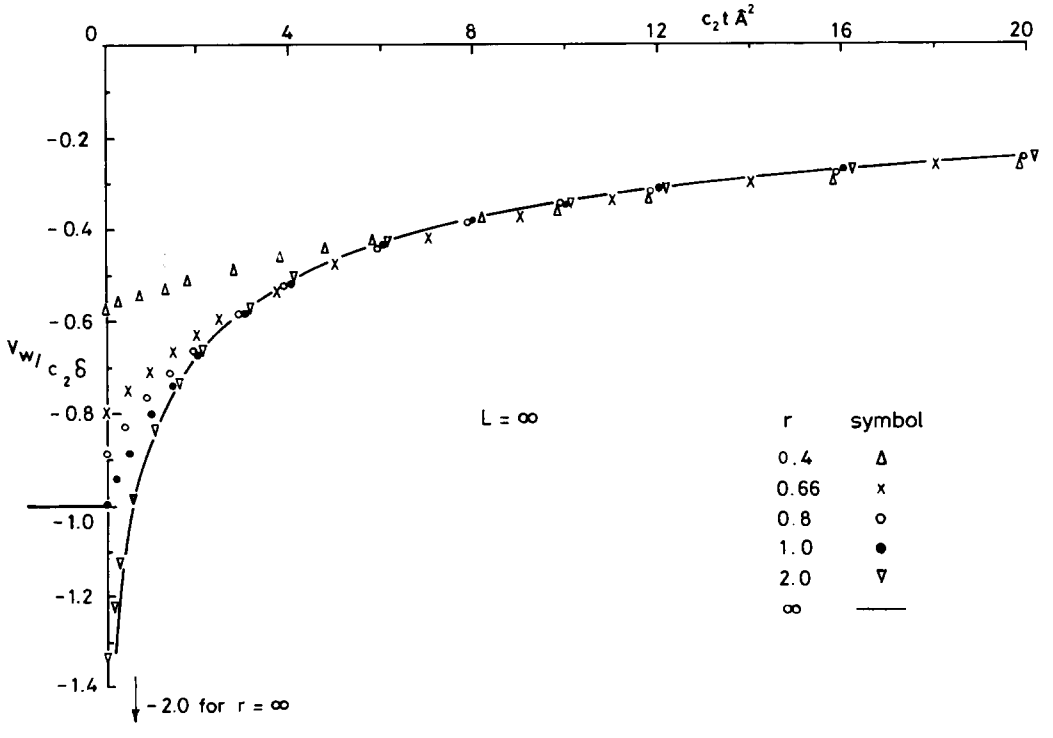

Figure 2. The influence of inertia on inflow velocity v_w versus time t at early times after the impact of I on the interface at $y = 0$. The full line ($r = \infty$) illustrates behaviour for the case of no inertia; the number r is related to the "openness-ratio" of the interface (see Sec. 3 for details).

enables one to appreciate the role of the inertia of the air within the tubes in a very direct way. For example, one can see from Fig. 2 that the major effect occurs for early times after shock reflection and is such as to reduce the rates of inflow. It can also be seen that at later times inertia has the effect of sustaining the inflow by a small, but nonetheless noticeable, amount.

(ii) The case L finite

When L is finite the simplification afforded by the replacement of $\tanh(\bar{\alpha}L(z(z+1))^{1/2})$ by unity in (4.2) is no longer available. Furthermore there are no special values of r that lead to a reduction in the task of evaluating (4.2), save for the limiting case $r=\infty$. One must remember that $r=\infty$ only has physical relevance as a limiting quantity in the particular circumstance that allows ρ_c to shrink to a limitingly small value; these conditions have already been discussed in Sec. 3 so that we already know that the earlier "inertia-less" model is recovered under these conditions. It should be noted that the finite-L situations encountered in this earlier "inertialess" model of behaviour could also only be evaluated by numerical means (Clarke [3]). Evidently one must face up to the task of a detailed evaluation of the features of the integral in (4.2), with parameter r in the range $0<r<\infty$. The issue is quite a complicated one and it is advantageous to limit discussion to the finite range $0<r\leqslant 1$, which is the practical one encountered in shock-tube experiments. When r is zero V is equal to unity and (3.1) and (4.1) show that v_w is zero, as it should be for a completely closed surface at $y=0-$.

There is some small advantage to be gained from re-writing (4.2) as

$$V-1=-\frac{1}{2\pi \mathrm{i}}\int_{Br}\frac{2\exp(c_2t\bar{\alpha}z)}{z+r^{-1}(z(z+1))^{1/2}\coth\left(\bar{\alpha}L(z(z+1))^{1/2}\right)}dz, \tag{4.9}$$

and some effort will have to be devoted to an understanding of the character of the integrand in this equation. Writing $z=\xi+\mathrm{i}\eta$ (ξ, η real) the main features of the integrand can be summarised here as follows: The integrand has no branch points, and no singularities of any kind in $\xi>0$. There are no singularities in $\xi\geqslant-\frac{1}{2}$, $|\eta|>0$, but poles may occur on $\eta=0$, $\xi<0$. If $\bar{\alpha}L$ is large enough for any given r, poles may occur in $-\frac{1}{2}<\xi<0$, $\eta=0$. A denumerable infinity of complex-conjugate poles exists in the domain $\xi<-\frac{1}{2}$. Their distance apart in the η-direction is very roughtly $\pi/\bar{\alpha}L$. For example when $r=\frac{2}{3}$ and $\bar{\alpha}L=2$ (or $\hat{A}^2L=4.5$) the first pair of poles lies at $(-0.8957, \pm 2.1694)$ in the z-plane and the next pair at about the same ξ value and $\eta\simeq\pm 3.82$.

Evidently the contour Br can be closed on its left-hand side, and $(1-V)$ therefore written as the sum of the residues at the poles of the integrand of (4.9). Since it is a tedious matter to locate a sufficient number of conjugate poles of the type that have just been described, and since there is no ready way to check upon the rate of convergence of the associated infinite sum, this procedure has not been attempted here. However the investigation of the character of (4.9) is not in vain since it has exposed the existence of conjugate poles in $\xi<0$ and, in addition, poles on $\eta=0$ in $-\frac{1}{2}<\xi<0$, the latter for sufficiently large values of $\bar{\alpha}L$. In such circumstances it is possible to use (4.9) to obtain an estimate of the way in which $(V-1)\to 0$ as $c_2t\bar{\alpha}$ increases, since the contribution from a pole in $-\frac{1}{2}<\xi<0$ will predominate over the contributions from the sequence of

conjugate poles. The general analysis demonstrates that v_w will always approach zero as t increases without bound, although to find the way in which it does so will be quite complicated if, as is possible, $\bar{\alpha}L$ is too small to admit the presence of a pole in $-\frac{1}{2} < \xi < 0$ when $\eta = 0$.

It is useful to revert to (4.2) and to reorganise the terms in { } as follows:

$$\{\quad\} = \left[Q(z) + \mathrm{e}^{-2I(z)}\right]\left[1 + Q(z)\mathrm{e}^{-2I(z)}\right]^{-1}, \tag{4.10}$$

where

$$Q(z) \equiv \left((z+1)^{1/2} - rz^{1/2}\right)/\left((z+1)^{1/2} + rz^{1/2}\right), \tag{4.11a}$$

$$I(z) = \bar{\alpha}L(z(z+1))^{1/2}. \tag{4.11b}$$

Expanding the final bracket term in (4.10), as is permissible when $\mathrm{Re}\, z = \xi$ is large and positive for example, (4.2) can be written as

$$V = \frac{1}{2\pi \mathrm{i}} \int_{Br} \frac{1}{z} \Bigg\{ Q(z) + \left[1 - Q^2(z)\right] \exp(-2I(z)) + \sum_{n=2}^{\infty} (-1)^{n-1} Q^{n-1}(z)\left[1 - Q^2(z)\right] \exp(-2nI(z)) \Bigg\} \mathrm{e}^{c_2 t \bar{\alpha} z} dz. \tag{4.12}$$

The index $-2I(z)$ behaves like

$$-2\bar{\alpha}Lz - \bar{\alpha}L + (\bar{\alpha}L/8z) + \ldots$$

as $|z| \to \infty$, so that (4.12) gives rise to an unending sequence of terms that vanish when $c_2 t\bar{\alpha} < 2n\bar{\alpha}L$, $n = 1, 2, 3, \ldots$, except for the first term which, from the definition of $Q(z)$ in (4.11a), can be seen to be exactly V_∞, defined in (4.4).

Thus, in the interval $0 < c_2 t\bar{\alpha} < 2\bar{\alpha}L$, V behaves just as if the length of the slender tubes is unbounded. At $c_2 t = 2L$ their finite depth becomes apparent in the shape of a disturbance that has clearly reflected from the closed lower surface at $y = -L$, and this is followed by the unending sequence of further reflections at $c_2 t = 2nL$, $n = 2, 3, \ldots$.

The amplitude of the jump that occurs in V at $c_2 t = 2L$ is readily seen to be equal to

$$4r(1+r)^{-2} \exp(-r^2 \hat{A}^2 L), \tag{4.13}$$

with subsequent jumps of amplitude

$$(-1)^{n-1} 4r(1+r)^{-2}\left[(1-r)/(1+r)\right]^{n-1} \exp(-nr^2\hat{A}^2 L), \quad n = 2, 3, \ldots. \tag{4.14}$$

Since $0 < r \leqslant 1$ it is clear that the amplitude of each jump is less than unity, even in the physically unlikely situation for which $\hat{A}^2 L \to 0$. However it is interesting to observe how slowly $4r(1+r)^{-2}$ diminishes with diminishing value of r; when $r = 1$ it is unity, when $r = \frac{2}{3}$ it is 0.96 and when $r = \frac{1}{3}$ it is still as large as 0.75.

It can be seen that the set of curves of $v_w/c_2\delta$ versus $c_2t\hat{A}^2$ presented in Fig. 2, for $L = \infty$ and a variety of values of r, are now valid for any value of L for c_2t up to but not exceeding $2L$. At this value of c_2t a jump in $v_w/c_2\delta$ of magnitude (4.13) occurs, as illustrated in Figs. 3 and 4 for the two cases $r = \frac{2}{3}\&1$, and four values of $\hat{A}^2L$ (or $\bar{\alpha}L$, $= r^2\hat{A}^2L$). The value unity for r is strictly not achievable when (3.10b) holds on purely

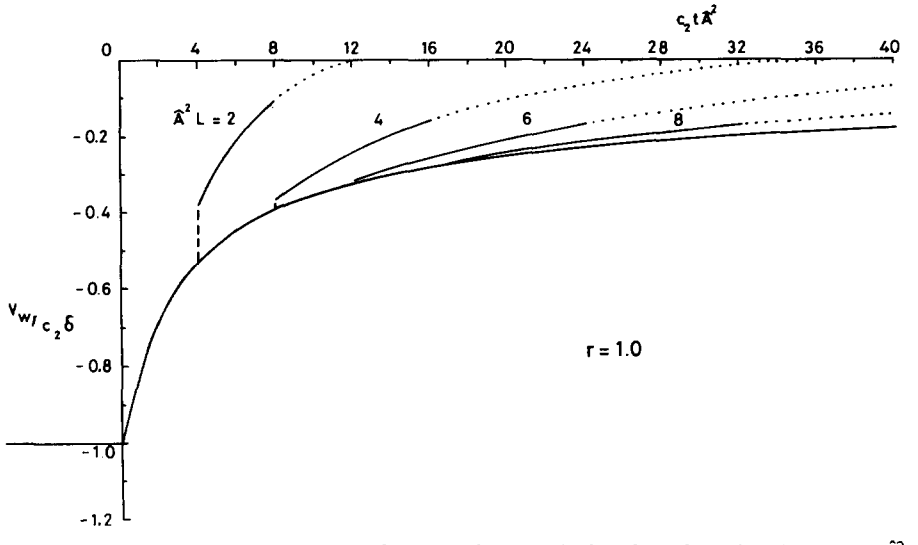

Figure 3. Inflow velocity v_w versus time t for four values of tube-length L when r is unity. For $c_2t\hat{A}^2$ between zero and the first jump the inflow takes place as if into tubes of infinite length. The jump in v_w is the result of the first reflected wave for tubes of finite length and is always a compression. Subsequent jumps alternate in sign; they do not show up on the scale of this Figure but the first small expansive jump is visible in Fig. 4 for $\hat{A}^2L = 2\&4$. The dotted curves are explained in Sec. 5, paragraph five.

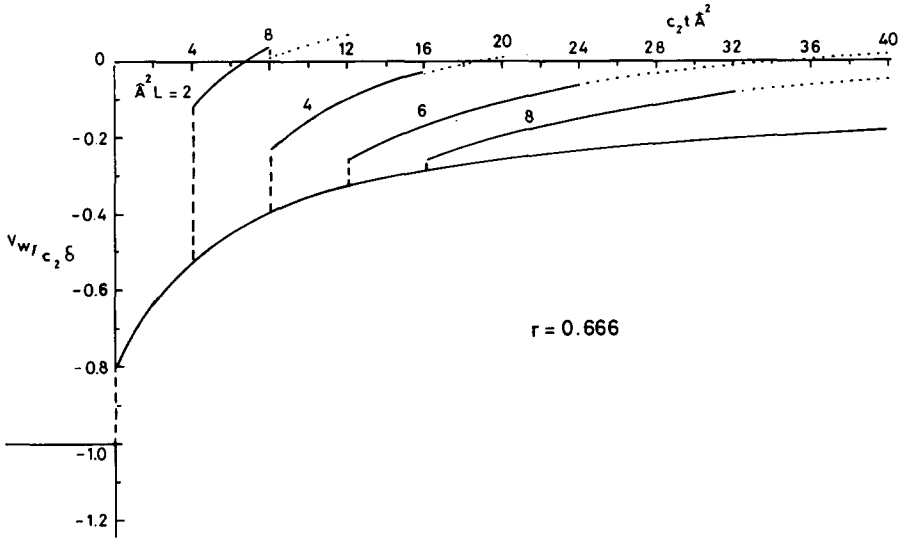

Figure 4. Inflow velocity v_w versus time t for four values of tube-length L (as in Fig. 3) when r is equal to two-thirds.

practical grounds for holes of circular cross-section; one might visualise a set of square holes separated by walls of vanishing thickness but again this is hardly practical, and one would have to reinterpret the meaning of a too. Reverting to (3.10a) it is logical to assert that ρ_c and ρ_2 should be approximately the same, but c could be significantly smaller than c_2 if the walls of the slender tubes are distensible under the action of the over-pressures within them, as can be seen from §2.1 of Lighthill's [5] book, especially equation (10) there. At all events $r = 1$ is a useful limiting value to exploit.

5. Discussion

Consider Fig. 3, which depicts v_w versus $c_2 t\hat{A}^2$ for $r = 1$, at least for $0 < c_2 t < 4L$. Note that the jumps in the v_w curve that occur at $c_2 t = 2L$ are of rapidly diminishing amplitude as L increases, as is evident from a glance at (4.13).

When incident shock wave I initiates motion in the thin tubes the signal is transmitted towards the closed end of these tubes at $y = -L$ as a jump in pressure, flow velocity, etc., that travels at the sound speed c_2. (To see this one needs to revert to the equations in Section 2 so as to derive a relation between the average velocity within a tube and the pressure at its open end; the result just quoted then follows and shows that, in general, discontinuous wave-fronts propagate back and forth between $y = 0$ and $-L$). When the surface is "fully-open", and $r = 1$, each tube initially swallows the whole incident shock; this pressure-jump travels to $y = -L$, where it is reflected and propagated back towards $y = 0$, suffering viscous attenuation throughout the process. A jump of pressure or velocity v_w emerges at $c_2 t = 2L$ which is therefore much weaker than the initial input value from I. This can be clearly seen on Fig. 3, where the *magnitude* of the input-value of $v_w/c_2\delta$ is one and the magnitude of the largest jump (at $c_2 t\hat{A}^2 = 4$ for $\hat{A}^2 L = 2$) is about 0.14. As L increases this latter quantity diminishes very significantly and the effect is, for all practical purposes, more like a simple change in the slope of $(v_w/c_2\delta)$ versus $(c_2 t\hat{A}^2)$ for $\hat{A}^2 L \geq 6$. Of course r cannot be as large as unity in a practical situation, but the limit is useful as a comparator, as discussed at the end of Sec. 4.

When the surface is partly closed, as it is when $r = \frac{2}{3}$, the situation is *qualitatively* the same, but noticeably different quantitatively speaking, as can be seen in Fig. 4. Since I reflects directly from $y = 0$, in part at least, for all $r < 1$ the pressure-signal that drives flow into the porous material is initially *stronger* than is the case when $r = 1$; thus, as can be seen from Fig. 4, the emergent jumps of velocity (or pressure) when $r < 1$ are larger than the jumps that appear when $r = 1$ for the same length of tube.

Equation (4.14) shows that the *sign* of consecutive reflections alternates, as indeed one would suspect that it should when the inertia of the airflow in the tubes is taken into account, along with its capacity to cause the flow to "overshoot" its equilibrium configuration. The character of the integrand in (4.9) allows one to deduce that this equilibrium state is the one for which v_w is zero, and both external and internal (to the tubes) pressures are finally equalised.

The curves in Fig. 3 and 4 that follow after the jumps at $c_2 t = 2L$ are calculated numerically from the second term in the integral in (4.12). The dotted extensions beyond $c_2 t = 4L$ are continuations of this same expression beyond the appearance of the first reflected wave. The only exceptions occur for the two cases $\hat{A}^2 L = 2\&4$ in Fig. 4 where the jump, calculated from (4.14), has been subtracted from the sum of the first two terms of (4.12). It is evident from the case $\hat{A}^2 L = 4$ that the jump is of no real practical significance

for any higher L values and, accordingly, we regard the situations depicted in Figs. 3 and 4 as adequate approximate summaries of the true physical situation.

It can be seen from (3.1) and (3.2) that a positive value of $v^{(1)}$ or, equivalently, a value of $v_w/c_2\delta$ greater than -1 implies a positive increment of pressure above the post-incident-shock value of pressure, namely p_2. Thus Figs. 3 and 4 can also be interpreted as a history of the compression waves emanating from the interface at $y = 0$. Equations (3.3) and (3.4) summarise the character of the weakly non-linear field that will exist in the gas above $y = 0$ for all times greater than zero (equivalently, $\beta > 0$) except for the insertion of shock-waves which may be required to prevent the occurrence of multiple values of $v^{(1)}$, $p^{(1)}$ etc. For example, the sudden jumps at $t = 0$ and $4\hat{A}^2/c_2$ when $r = \frac{2}{3}$ (Fig. 4) demand the appearance of shocks immediately, at $y = 0$, at these times. For intermediate and subsequent times the slow compressions that are evident throughout Figs. 3 and 4 will lead to a steady strengthening of the shocks at their head. There is no obstacle to prevent one from fitting shocks into the field in $y > 0$, by exploiting the equal-areas rule for example (Whitham [7], §2.8). It is not done here because the purely qualitative character of the outcome is quite evident from Figs. 3 and 4, and this is sufficient for present purposes.

The present analysis has revealed as much as one needs to know at this stage; the influence of inertia, viscosity, tube-length, etc. can now be appreciated, and the relevant parameter-groups have been exposed. In conclusion it is interesting to observe that the positive values of $v_w/c_2\delta$ that are evident on Fig. 4 for $c_2t\hat{A}^2 > 4$, mean that the strength of the reflected shock wave from the perforated end-plug will *exceed* the strength of the shock reflected from a solid wall, at some time after the initiation of reflection, and before finally subsiding to the same solid-wall value. The only satisfactory way to ensure that an undesirable overshoot of this kind does not occur is to make the tubes long enough, as can be seen from Fig. 4, for example.

Scott's [6] observation of the flow in the reflected-shock domain for a configuration like the one sketched in Fig. 1 make an interesting post-script to the foregoing theory. As described in the Introduction, his main objective was the generation and observation of the behaviour of fully-dispersed shock waves in carbon dioxide. As part of the process of understanding the interaction between the flow generated behind the incident wave I and the perforated plug Scott made measurements with air as the working gas and, to the extent that relaxation processes are essentially absent in this case, these observations are comparable with the present theory. Copies of two pressure-time histories are exhibited here in Figs. 5a and b. They have been annotated to show the values of p_1, p_2 and p_3, where the first two pressures are defined in Fig. 1, and p_3 is the value of pressure after reflection of I from a solid wall. The measurements were made at a distance of 36.5 mm above the air/perforated-plug interface, with an incident-shock Mach number of 1.66 and 1.68 in the two cases. The value of the perturbation-number δ, defined in Fig. 1, is about 0.74 in these circumstances, so that comparisons between Scott's observation of a strong disturbance field and the present theory's account of weak disturbance behaviour can only be of a qualitative character. The plug used in the experiments contained sixty-four holes of diameter 2.38 mm and length either 88.9 or 28.1 mm (Figs. 5a and b, respectively). With a square tube cross-section of side 45 mm this gives a value for σ of 0.141. With such a large tube diameter the estimated value of $\bar{\alpha}$ (which, from (2.1) and (4.3), is given by $8\nu_2/a^2c_2$ in the present theory) is small, roughly 0.005 cm^{-1}. The use of (2.1) to estimate the viscous resistance to flow in the slender tubes implies that this flow is laminar; Scott's observations suggest that this may not be so, and that flow in the tubes may be turbulent in character. Even if one adopts the rather crude expedient of simply increasing the value

of the viscosity in α (see (2.1)) to account for this fact it is not reasonable, physically, to imagine that $\bar{\alpha}$ will be increased by more than a factor of ten, so that $\bar{\alpha}$ appears to be essentially small for Scott's experiments. It may be rather more reasonable to assume that the realities of the experimental set-up can be represented by a type of "discharge-coefficient" reduction in the factor σ (or r), since this certainly results in the lower mass-flux rates into and out of the plug that intuition suggests may prevail in the case of the strong disturbances produced in the experiments.

When $\bar{\alpha}$ or, equivalently, $r^2\hat{A}^2$ (see (4.6)) is small the changes that take place in the inflow factor V with changing time are also small for time intervals between the jumps whose magnitudes are given in (4.13) and (4.14). This can be seen by consulting (4.12) for example and remarking that $c_2 t\bar{\alpha}$ remains reasonably small for $0 < c_2 t\bar{\alpha} <$ (say) $4\bar{\alpha}L$,

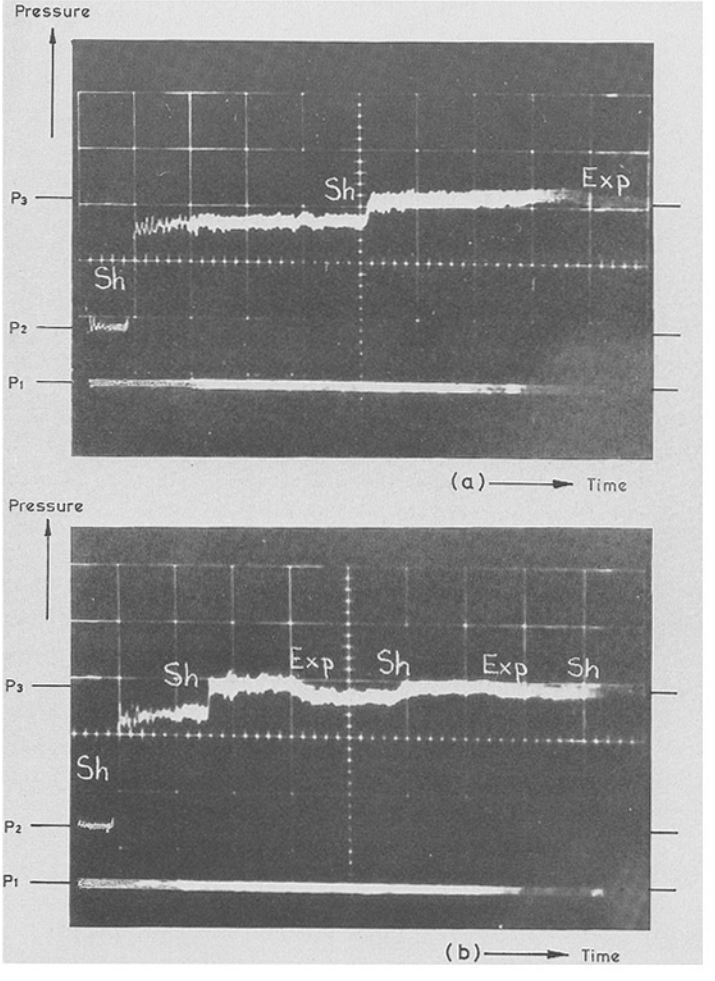

Figure 5. Pressure versus time measured in the reflected wave field by E.M. Scott [6]; reproduced from his Figures 3.4.7, C&D. (a) Incident shock Mach number = 1.66, $p_1 = 200$ torr, $L = 88.9$ mm. (b) Incident shock Mach number = 1.68, $p_1 = 200$ torr, $L = 28.1$ mm. The value of $p_3 - p_1$ is calculated from the measured $p_2 - p_1$ value and the formula for the pressure-ratio of a shock reflected from a solid wall (e.g. Equation (70.05), page 153, in *"Supersonic flow and shock waves"*, R. Courant & K.O. Friedrichs, Interscience, New York, 1948); this formula is known to agree very well with observations.

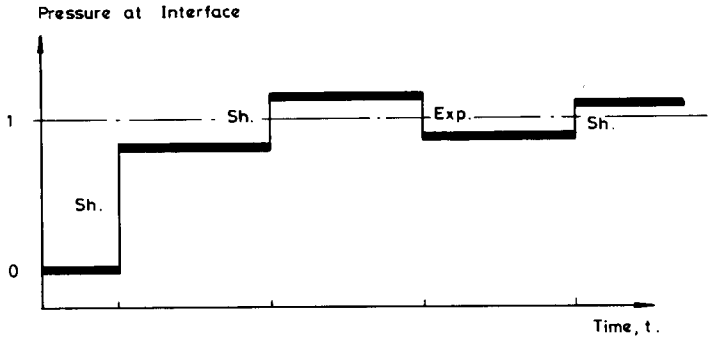

Figure 6. Pressure variations at the air/perforated-plug interface after reflection of the incident shock, according to the present theory with $r = 0.1$ and $\bar{\alpha} = 0$. *Sh* and exp denote shocks and expansion-waves in the reflected wave field.

since $4\bar{\alpha}L$ is itself small. The effect of the small changes in the magnitude of the exponential factor $\exp(c_2 t\bar{\alpha}z)$ on the value of the integrals (see (4.7) for example) is clearly not large under these conditions.

Thus, in rough terms, the present theory predicts that when r and $\bar{\alpha}$ are small the inflow factor V will behave as a sequence of steps, as illustrated in Fig. 6 for $r = 0.1$ and $\bar{\alpha} = 0$. In view of (3.2) and the definition of V in (4.1) it is clear that the ordinate in Fig. 6 can be labelled as a pressure, evaluated at the interface; the value zero on the figure corresponds with p_2 on Fig. 1 and unity indicates the asymptotic value of pressure behind the reflected waves, which we have already seen (in Sec. 4) must correspond with the no-inflow ($v_w = 0$) solid-wall value p_3.

Remembering that the centred expansion wave, labelled Exp. on Fig. 6, will have spread out by the time it reaches the measuring station in Scott's experiments, the comparison between Figs. 5 and 6 reveals as satisfactory a degree of agreement between theory and observation as one is entitled to expect in the circumstances.

Acknowledgement

The author is grateful to the Procurement Executive of the Ministry of Defence for their financial support of the work described above.

References

[1] M. Abramowitz and I.A. Stegun, *Handbook of mathematical functions*, Dover, New York (1965).
[2] J.F. Clarke, The reflection of weak shock waves from absorbent surfaces, *Proc. R. Soc. Lond.* A, (in the press).
[3] J.F. Clarke, Regular reflection of a weak shock wave from a rigid porous wall, *Quart, J. Mech. Appl. Math.*. 37 (1984) 87–111.
[4] A. Erdélyi, W. Magnus, F. Oberhettinger and F.G. Tricomi, *Tables of integral transforms, Vol. 1,* McGraw-Hill Book Co. Inc., New York (1954).
[5] M.J. Lighthill, *Waves in fluids*, Cambridge University Press (1978).
[6] E.M. Scott, *Weak compression waves in relaxing gases*, Ph.D. Thesis, Cranfield Institute of Technology, Cranfield, England (1972).
[7] G.B. Whitham, *Linear and nonlinear waves,* John Wiley and Sons, New York (1974).